Synthesis and radical coupling of pyridine-bridged π-extended tetrathiafulvalene (TTF)-type donors and push–pull analogues

Eva M. Priego,[a] **Luis Sánchez,**[a] **M. Angeles Herranz,**[a] **Nazario Martín,***[a] **Rafael Viruela**[b] **and Enrique Ortí***[b]

Received 5th February 2007, Accepted 26th February 2007
First published as an Advance Article on the web 20th March 2007
DOI: 10.1039/b701806a

A new family of π-extended TTF analogues (**3a–c**) and D–π–A chromophores (**5a–c**), in which the electroactive units (1,3-dithiole rings and 2,2-dicyanovinyl groups) are connected through a pyridine bridge with a *meta* substitution pattern, is reported. The redox behavior of these compounds has been investigated by cyclic voltammetry and theoretical calculations performed at the B3P86/6-31G** level. Unlike many π-extended TTF derivatives, the 1,3-dithiole rings in compounds **3a–c** do not behave independently and two oxidation processes are observed with an anodic separation ranging from 50 to 150 mV. Calculations show that electrons are equally extracted from both dithiole rings. A biradical structure is predicted for the dication state due to the near-degeneracy of the HOMO and HOMO − 1 orbitals. The presence of both donor (D) and acceptor (A) fragments in conjugates **5** results in irreversible oxidation and reduction processes associated with the 1,3-dithiole ring and with the 2,2-dicyanovinyl moiety, respectively. An electrochemical–chemical–electrochemical (ECE) process takes place for all the compounds reported. The chemical process implies the dimerization of the radical cation for compounds **5** and the oligomerization of the biradical dication for compounds **3**. The ECE process therefore generates new neutral dimeric (**5**) or oligomeric (**3**) species that incorporate the TTF vinylogue core.

Introduction

The construction of nanosized devices and machines, capable to be developed for different functions like data storage, signal processing, *etc.*, represents a key stage in the miniaturization process required for the implementation of the so-called *molecular electronics*.[1] Although illustrative examples of such devices at nanoscale dimensions, like molecular wires,[2] logical gates,[3] switches[4] and organic field effect transistors (OFETs),[5] have been successfully reported, further investigations about important parameters like redox properties, conjugation, molecular size and geometry of the molecular components are required.[6] The processes involved in the correct operation of molecular electronic devices, such as electron transfer/transport or n-/p-doping, are strongly influenced by these parameters. Molecular geometry conditions the assembly and orientation of the molecules in the solid state and thereby the properties of the devices.[7] The conjugation length of the constituent materials is directly related to their redox behaviour because it determines the energy position of the HOMO/LUMO levels and, hence, the electron-donating and/or electron-accepting properties.

In order to achieve good electron-donor and electron-acceptor abilities within a readily accessible potential window, *i.e.* a low HOMO–LUMO gap, two different synthetic strategies are being used: *i*) the extension of π-conjugation and *ii*) the coupling in the same molecule of both donor (D) and acceptor (A) fragments linked by different chemical spacers.[8] Whereas conjugated polymers exemplify the success of both strategies,[9] obtaining such an amphoteric redox behaviour has been a hard challenge in small organic molecules. Oligoacenes and σ-/π-linked D–A ensembles, including fullerene materials, exemplify the first and the second approaches, respectively.[8]

The tetrathiafulvalene (TTF) molecule, firstly reported by Wudl more than three decades ago,[10] represents a paradigmatic case of a chemical building block to attain molecules bearing narrow HOMO–LUMO gaps.[8,11] Different research groups have been actively working on the synthesis of TTF derivatives by applying both of the above mentioned strategies. A wide variety of π-extended TTF systems, where conjugated vinylene units,[12] five-membered heterocycles[13] and quinoid acenes[14] have been used as conjugated units bridging the two 1,3-dithiole rings of TTF, exemplify the first strategy. In most of these examples the extension of the π-system renders a smaller HOMO–LUMO gap.

TTF as well as its *p*-quinoid congeners have been chemically modified to generate several families of TTF–bridge–A conjugates. The nature of the chemical spacer can be modified by using well-established synthetic methodologies and the properties of the final TTF–spacer–A assemblies stem directly from the nature of the linker unit.[15] Interfacing TTF or π-extended TTFs with different acceptor fragments separated by π-conjugated spacers, like multiple C–C bonds or aromatic rings, give rise to D–π–A push–pull structures exhibiting second-order nonlinear optical (NLO) properties, which hold promise in optoelectronics and all-optical data processing technologies.[16] The NLO properties of this kind of compounds can be tuned introducing different electron-acceptor fragments like dicyano- and tricyanovinylene units,

---

[a] *Departamento de Química Orgánica, Facultad de Química, Universidad Complutense, 28040, Madrid, Spain. E-mail: nazmar@quim.ucm.es; Fax: +34 91 3944103; Tel: +34 91 3944227*

[b] *Institut de Ciència Molecular, Universitat de València, ES 46980, Paterna, Spain. E-mail: Enrique.orti@uv.es; Fax: +34 963543274; Tel: +34 963544438*

barbituric derivatives or tricarbonyl chromium arene complexes to name a few.[17] Molecules endowed with only one 1,3-dithiole ring as D unit and connected by a π-spacer to an A moiety have been reported as useful prototypes for NLO materials despite their weaker electron-donor character.[18]

In the quest for new TTF prototypes bearing enhanced electronic and geometrical features we report herein on the synthesis of a new family of pyridine-bridged π-extended electron donors (**3a–c**) and push–pull chromophores (**5a–c**), in which both electroactive units, *i.e.*, the 1,3-dithiole rings or the 2,2-dicyanovinyl fragment, are in a relative *meta* position. Recent studies on *meta*-linked phenylacetylene derivatives have shown that whereas the *meta* linkage leads to electronic decoupling of the electroactive groups in the ground state, an enhanced electronic coupling results in the excited state.[19] As a consequence, the bridge would act as a wire or a resistor when it is in its excited or ground electronic state, respectively. Furthermore, the presence of chlorine atoms on C-2 and C-6 positions of the pyridine ring could allow a further chemical functionalization or their incorporation in more complex systems.[20] The redox properties of pyridine-bridged π-extended-TTF donors (**3a–c**) and D–π–A chromophores (**4a–c** and **5a–c**) have been investigated by cyclic voltammetry. A detailed theoretical study on the geometry and the electronic properties at the density functional theory (DFT) level complements this work.

Results and discussion

Synthesis and molecular structure

The synthesis of the target compounds **3a–c** and **5a–c** (see Scheme 1) started from 2,6-dichloropyridine-3,5-dicarbaldehyde (**1**), which could be readily prepared in three steps by following the experimental procedure previously reported in the literature.[21] A Wadsworth–Emmons olefination protocol between the bis-aldehyde **1** and different stoichiometric ratios of phosphonate esters **2a–c**[22] led to pyridine-bridged π-extended donors **3a–c** or mono-aldehyde D–π–A dyads **4a–c** in moderate yields. The final step towards the π-conjugated D–A structures **5a–c** consisted in a Knoevenagel-type reaction by using malononitrile, acetic acid and ammonium acetate with azeotropic elimination of water.

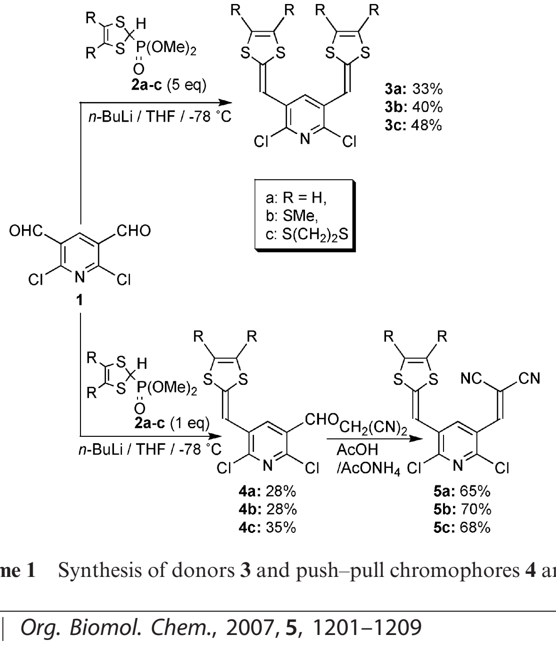

Scheme 1 Synthesis of donors **3** and push–pull chromophores **4** and **5**.

All the new synthesized compounds were unambiguously characterized by using analytical and spectroscopic techniques. For compound **3a**, diagnostic resonances at δ 7.85, 6.76, 6.48 and 6.38 in its ^{1}H NMR spectrum clearly support the proposed structure. The presence of the aldehyde functionality in compounds **4a–c** was confirmed by a band centered at 1700 cm^{-1} in the IR spectrum and a resonance at around δ 180 in the ^{13}C NMR spectrum. Analogously to **4a–c**, the IR spectra of compounds **5a–c** are indicative of the proposed structures since the characteristic band at around 2225 cm^{-1} due to the stretching vibration of the cyano groups could be observed. In addition, a new set of resonances at $\delta \sim 8.1$ corresponding to the vinylic proton of the 2,2-dicyanovinyl unit appeared in the ^{1}H NMR spectra of **5a–c**.

The molecular structure of compounds **3–5** was theoretically investigated by performing DFT calculations at the B3P86/6-31G** level. DFT calculations include correlation effects at a relatively low computational cost and are known to provide accurate equilibrium geometries.[23]

The molecular structure of **3a** was optimized under different symmetry restrictions. The minimum-energy conformation corresponds to the C_2 structure sketched in Figs. 1a and 1b, in which the dithiole rings are twisted by 21.3° around the C2–C3 bonds (see Fig. 1a for atom numbering) and are situated slightly above and below the plane of the pyridine ring. The resulting structure is calculated to be 0.64 kcal mol^{-1} more stable than the fully planar C_{2v} structure, in which the S5 atoms are at a shorter distance of 3.68 Å and, is almost isoenergetic ($\Delta E = 0.18$ kcal mol^{-1}) of the C_s conformation in which both dithiole rings lie above the pyridine plane. For compound **5a** (Fig. 1c), the dithiole ring and the C(CN)$_2$ group adopt a *cis* orientation and prefer to be situated on the same side of the pyridine plane. This is due to the stabilizing electrostatic interaction between the positively charged S5 atom (+0.43e) and the negatively charged N10 atom (−0.31e) situated at 3.22 Å. Atomic charges were calculated using the natural population analysis (NPA) approach.

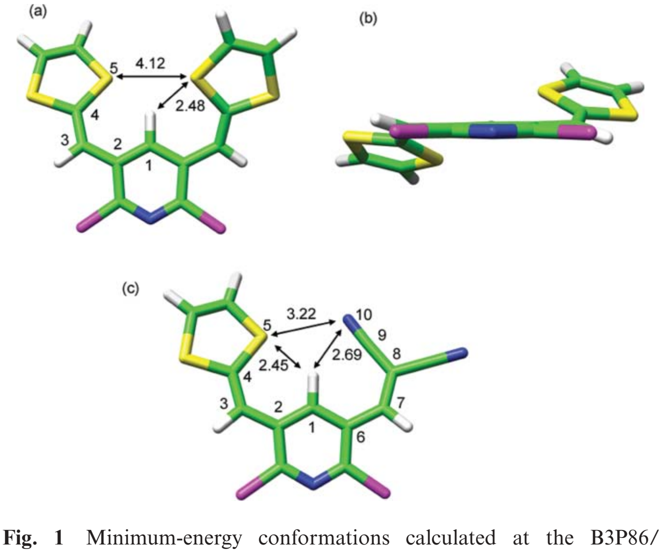

Fig. 1 Minimum-energy conformations calculated at the B3P86/6-31G** level for **3a** [top view (a) and side view (b)] and **5a** (c). Interatomic distances are given in Å. Atomic numbering is also indicated.

Electronic characterization

Despite the π-deficient character of the pyridine spacer, the electronic spectra of compounds **3a–c** maintain high resemblance to the spectra of other previously reported π-extended TTF-based electron donors and show a strong absorption at $\lambda_{\max} \approx$ 370–400 nm (Fig. 2). The absence of a low-energy band in the visible region of the spectrum is indicative of a highly energetic HOMO–LUMO gap. In contrast, the weak bands observed in the 500–600 nm range for compounds **4a–c** and **5a–c** suggest an electronic interaction between the 1,3-dithiole ring, acting as electron donor, and the aldehyde or 2,2-dicyanovinyl moieties, acting as electron acceptors.

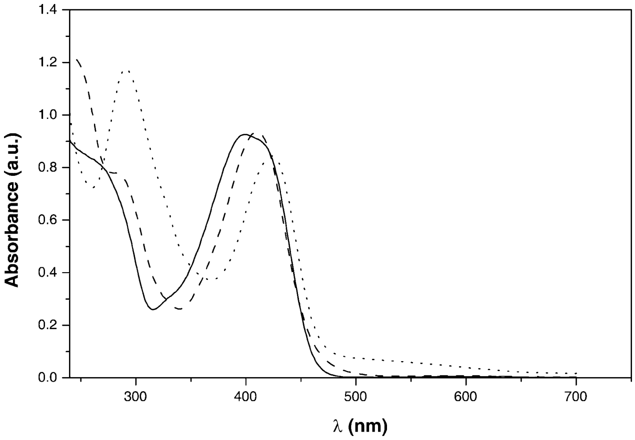

Fig. 2 UV/Vis absorption spectra of derivatives **3c** (solid line), **4c** (dashed line) and **5c** (dotted line) in CH_2Cl_2.

Fig. 3 shows the atomic orbital (AO) composition of the highest-occupied molecular orbitals (HOMO and HOMO − 1) and the lowest-unoccupied molecular orbitals (LUMO and LUMO + 1) of **3a**. The HOMO spreads over the whole molecule and results from the antibonding interaction of the HOMO of the pyridine moiety with the HOMOs of the 1,3-dithiol-2-ylidene units. The HOMO − 1 is symmetric and is localized over the 1,3-dithiol-2-ylidene groups. The LUMO and LUMO + 1 correspond to the LUMO and LUMO + 1 of pyridine antibondingly and bondingly interacting with the LUMOs of the 1,3-dithiol-2-ylidene units.

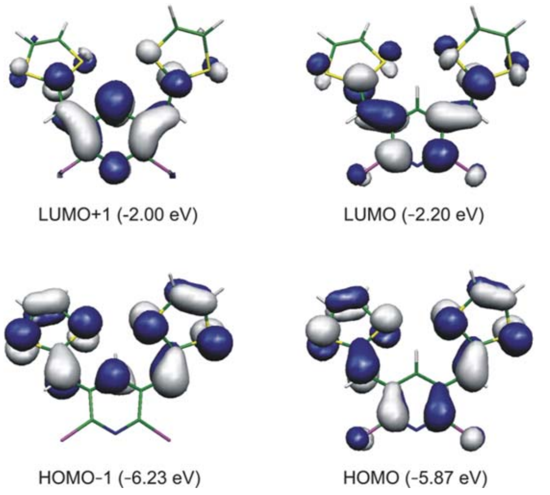
LUMO+1 (-2.00 eV)
LUMO (-2.20 eV)
HOMO-1 (-6.23 eV)
HOMO (-5.87 eV)

Fig. 3 Electron density contours (0.03 e $bohr^{-3}$) and energies (within parentheses) calculated for the frontier orbitals of **3a**.

To investigate the nature of the electronic transitions that give rise to the absorption bands experimentally observed in the UV-visible spectra, the electronic excited states of compounds **3** were calculated in CH_2Cl_2 by using the time-dependent DFT (TDDFT) approach, the B3P86/6-31G** optimized energies and the polarized continuum model (PCM) to take into account the interaction with the solvent. Calculations predict that the absorption band observed around 400 nm (Fig. 2) is quite complex in nature since it involves the electronic transition to four different electronic states. As shown in Fig. 3, the HOMO and HOMO − 1 are close in energy and the same is found for the LUMO and LUMO + 1. One-electron excitations between these orbitals therefore give rise to four electronic excited states that are very close in energy. For compound **3c**, the electronic transitions to these states are calculated at 2.92 eV (424 nm, HOMO − 1 → LUMO), 3.04 eV (408 nm, HOMO → LUMO), 3.11 eV (399 nm, HOMO → LUMO + 1) and 3.32 eV (373 nm, HOMO − 1 → LUMO + 1) and have oscillator strengths (f) of 0.15, 0.26, 0.32 and 0.19, respectively. The occurrence of several intense electronic transitions at similar energies explains the broad shape of the absorption observed experimentally (see Fig. 2 for **3c**).

The energy and topology of the frontier orbitals are significantly different for compounds **4** and **5**. As shown in Fig. 4 for **5a**, whereas the HOMO is mainly localized on the 1,3-dithiol-2-ylidene unit, the LUMO extends over the electron-acceptor $C(CN)_2$ group and the pyridine ring, both orbitals being separated by more than 1.2 eV from the HOMO − 1 and LUMO + 1, respectively. This causes the fact that the absorption band observed at around 400 nm for compounds **4** and **5** now originates in the HOMO − 1 → LUMO and HOMO → LUMO + 1 excitations. For compound **5c**, these excitations give rise to two electronic transitions calculated at 2.97 eV (417 nm, f = 0.33) and 3.07 eV (403 nm, f = 0.15), in good agreement with the intense band observed at 422 nm (Fig. 2). On the other hand, the HOMO → LUMO one-electron promotion implies an electron-density transfer from the dithiole ring to the rest of the molecule and gives rise to a low-energy charge-transfer state. The electronic transition to this excited state has a low intensity (f = 0.02–0.04) and causes the appearance of the new weak absorption in the 480–600 nm range for compounds **4** and **5** (see Fig. 2). This absorption therefore corresponds to a photoinduced charge transfer from the 1,3-dithiole ring, acting as electron donor, to the aldehyde (**4**) or 2,2-dicyanovinyl (**5**) groups, acting as electron acceptors.

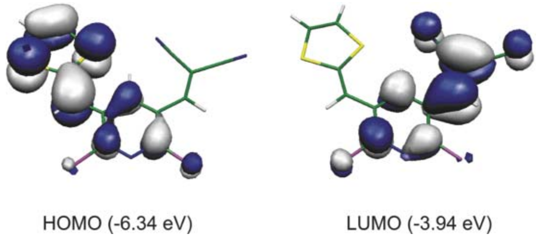
HOMO (-6.34 eV)
LUMO (-3.94 eV)

Fig. 4 Electron density contours (0.03 e $bohr^{-3}$) and energies (within parentheses) calculated for the frontier orbitals of **5a**.

Table 1 Oxidation and reduction peak potentials of donors **3a–c** and dyads **4a–c** and **5a–c** (CH_2Cl_2, in mV *vs.* $Ag/AgNO_3$)

Compound	E^1_{ox} [a]	E^2_{ox} [a]	E^1_{red} [b]	$E^{1/2}_{ox, oligomer}$ [c]
TTF[c]	+179	+530	—	—
exTTF[d]	+238	—	—	—
3a	+596	+750	—	+487
3b	+640	+729	—	+477
3c	+624	+673	—	+484
4a	+707	—	−1620	+455
4b	+732	—	−1567	+457
4c	+737	—	−1560	+457
5a	+708	—	−1010	—
5b	+727	—	−995	+495
5c	+735	—	−978	+499

[a] Irreversible oxidative processes, anodic peak potentials are reported. [b] Irreversible reductive processes, cathodic peak potentials are given. [c] Reversible oxidation processes, standard electrode potentials are reported. [d] 2-[9-(1,3-Dithiol-2-ylidene)anthracen-10(9*H*)-ylidene]-1,3-dithiole.

Redox properties

The electrochemical properties of the new pyridine-bridged π-extended donors **3a–c** and the π-conjugated D–A dyads **4a–c** and **5a–c** were studied by cyclic voltammetry (CV) at room temperature in dichloromethane solutions (see Table 1).

Donors **3a–c** show two irreversible oxidation peaks due to the oxidation of the 1,3-dithiole rings (see Fig. 5a for **3b**). The oxidation processes are shifted towards more positive potential values when compared with reference TTF or 2-[9-(1,3-dithiol-2-ylidene)anthracen-10(9*H*)-ylidene]-1,3-dithiole (exTTF) systems. Theoretical calculations predict that the HOMOs of TTF and exTTF are located at similar energies of −5.19 and −5.24 eV, respectively, whereas the HOMO of **3a** lies at −5.87 eV. This stabilization accounts, in a first approach, for the more positive oxidation potentials measured for compounds **3**. As expected, substitution on the 1,3-dithiole rings with the SMe or $S(CH_2)_2S$ groups leads to higher oxidation potentials and, thereby, to poorer electron-donor character.[14c] More interestingly, the two 1,3-dithiole rings do not behave independently despite the *meta* linkage and the extraction of the first electron from one of the 1,3-dithiole rings affects the second oxidation process, which appears positively shifted by 50–150 mV. As discussed below on the basis of theoretical calculations, both dithiole rings are indeed involved in the two oxidation processes.

Compounds **4a–c** and **5a–c** show one irreversible oxidation process due to the oxidation of the 1,3-dithiole ring. The oxidation potentials appear positively shifted when compared with donors **3a–c**, most probably due to the presence of the electron-withdrawing carbonyl or dicyanovinyl groups within the same structure. On the reduction side, an irreversible wave to form the radical anion is observed (see Figs. 5b and 5c for **4b** and **5b**, respectively). This reduction wave is anodically shifted in compounds **5a–c**, in comparison with their carbonyl containing precursors **4a–c**, due to the better acceptor ability of the 2,2-dicyanovinyl chromophore.[17a]

A closer inspection of the oxidative behaviour of these derivatives evidenced an interesting electrochemical–chemical–electrochemical (ECE) process. As discussed above, one (**4**, **5**) or two (**3**) irreversible oxidation peaks were observed on the first anodic scan. Upon successive scans, the intensity of these anodic peaks decreases and a new reversible redox system appears at remarkably lower oxidation potential values (see Fig. 6). This voltammogram shape indicates an ECE process: the initial electrochemical oxidation (E), corresponding to the oxidation of the 1,3-dithiole rings to the cation radical, is followed by a chemical reaction (C) leading to a new chemical species, which is further oxidized (E) at less positive potentials.

The above electrochemical mechanism has been previously reported for other related dithiafulvene derivatives[24,25] and has been thoroughly investigated by cyclic voltammetry.[26] For compounds **4a–c** and **5a–c**, the radical cation generated after the first electron transfer undergoes dimerization into a protonated dimer (see Scheme 2). Then, this protonated dication deprotonates into the non isolated TTF vinylogue (**6**), which is reversibly oxidized at lower potentials. The broad irreversible oxidation wave observed for **4a–c** and **5a–c** on the first scans indeed persists after 100 scans

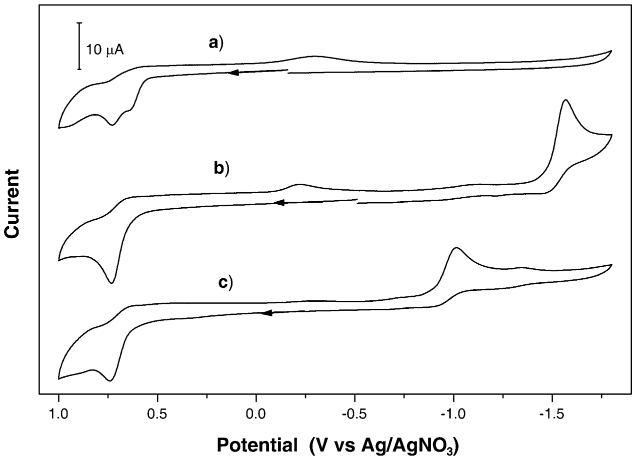

Fig. 5 Cyclic voltammograms for the pyridine-bridged π-extended donor **3b** (a) and for the dyads **4b** (b) and **5b** (c) in CH_2Cl_2 containing $TBAClO_4$ (0.1 M) as supporting electrolyte.

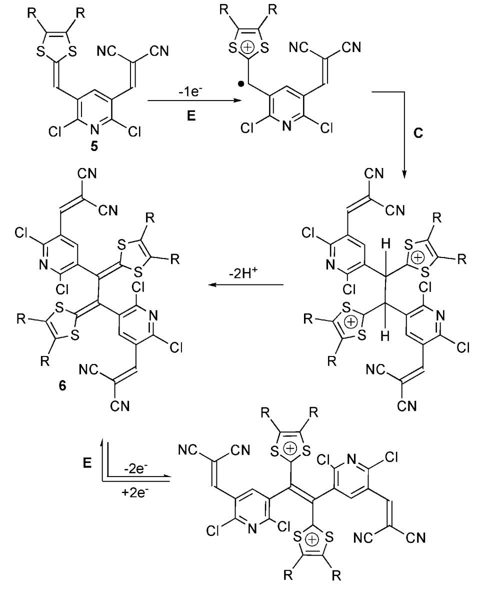

Scheme 2 ECE-Dimerization coupling proposed for push–pull chromophores **5**.

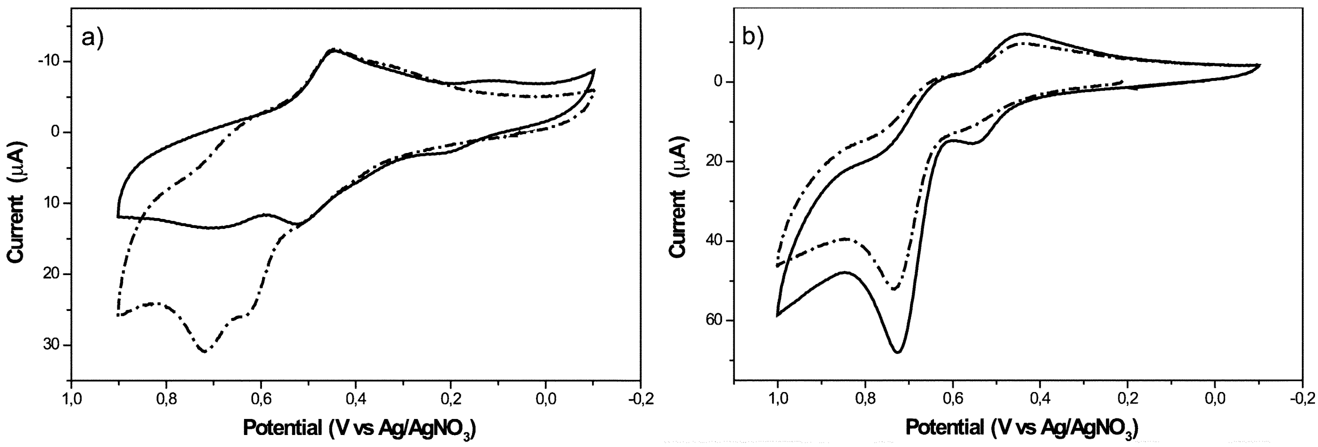

Fig. 6 a) Cyclic voltammogram of compound **3b** after one (dashed line) or 40 (solid line) scans. b) Cyclic voltammogram of compound **5b** after one (dashed line) or 40 (solid line) scans.

and coexists with the reversible oxidation wave emerging at lower values corresponding to the formation of the dimer.

For compounds **3a–c**, an oligomeric TTF vinylogue should be formed after successive oxidation–reduction scans due to the presence of two 1,3-dithiole-2-ylidene units. After 40 scans, the reversible wave corresponding to the oxidation of the oligomer species is the only one observed in the CV (see Fig. 6a). This contrasts with the behaviour of **4a–c** and **5a–c** and is due to the higher proportion of radicals that can be generated for compounds **3a–c**. From the half-wave oxidation potentials measured for dimeric and oligomeric species (see Table 1), the oxidation of these species appears to be almost insensitive to the nature of the substituents on the central spacer or on the 1,3-dithiole rings.

Oxidized/reduced species

Charged species (cations and dications for compounds **3** and cations and anions for **4** and **5**) were calculated to get a deeper understanding of the oxidation/reduction processes and to investigate how these processes affect the molecular structure and the electronic properties. Fig. 7 compares the optimized bond lengths calculated for **3a**, **3a**$^{\bullet+}$ and **3a**$^{2+}$.[27] Oxidation affects the whole molecule by modifying the lengths of the bonds in which the electron density in the HOMO (that is, the orbital from which electrons are removed) is concentrated. Only the bonds involving the pyridine nitrogen and the C1 atom remain almost unaffected because these atoms show no contribution to the HOMO (see Fig. 3).

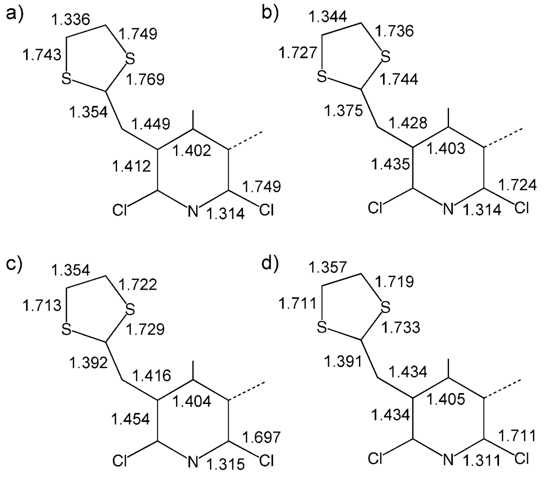

Fig. 7 B3P86/6-31G**-optimized bond lengths (in Å) calculated for a) **3a**, b) **3a**$^{\bullet+}$, c) **3a**$^{2+}$ (closed-shell singlet state) and d) **3a**$^{2+}$ (triplet state). All the species show a C_2 symmetry.

The electron in **3a**$^{\bullet+}$ is equally extracted from both dithiole rings, which remain twisted by 10.9° around the C2–C3 bonds and accumulate a net charge of +0.45e. All the attempts to find a localized structure, in which the electron was mainly removed from one dithiole ring, converged to the delocalized C_2 structure depicted in Fig. 7b. This result suggests that both rings are electronically linked through the pyridine ring and do not behave independently upon oxidation. This explains the occurrence of two separated oxidation processes in the CVs of compounds **3**, unlike many other π-extended TTF derivatives in which it is not possible to distinguish both oxidation processes.[14]

The dication of **3a** was first calculated as a closed-shell species in which both electrons are extracted from the HOMO. The resulting species (Fig. 7c) has an almost planar structure and accumulates a charge of +0.79e on each dithiole moiety. Taking into account that the HOMO and HOMO − 1 are close in energy for **3a** (Fig. 3), **3a**$^{2+}$ was recalculated as an open-shell triplet species in which one electron is removed from the HOMO and the other is extracted from the HOMO − 1. The dithiole rings in the resulting species (Fig. 7d) are twisted by 26.4° and have a charge of +0.89e each. The triplet dication is computed to be 7.43 kcal mol^{-1} more stable than the closed-shell singlet dication in CH_2Cl_2 (4.59 kcal mol^{-1} in gas phase). This result suggests that, upon oxidation to the dication state, the biradical species sketched in Fig. 8a is formed for compounds **3**. In contrast to **3a**$^{\bullet+}$, for which the unpaired electron is delocalized over both the dithiole and the pyridine rings, the unpaired electrons in **3a**$^{2+}$ are mainly localized on the dithiole environment with maximum spin densities of 0.49 at the vinylene C3 atoms. We have therefore to conclude that compounds **3** undergo the oxidative dimerization reaction to form TTF vinylogues at the dication stage. Compounds **3** would actually give rise to oligomeric TTF vinylogues, such as that depicted in Fig. 8b, because two positions involving the two radical species are liable to undergo coupling reactions. The formation of these oligomers is accounted for by the appearance of a new oxidation

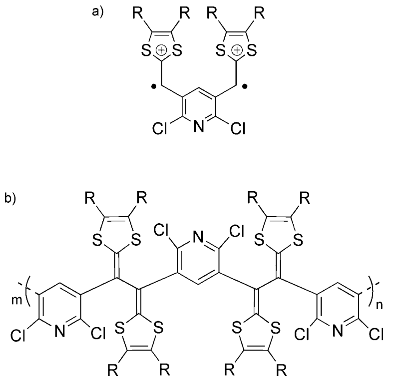

Fig. 8 a) Biradical structure of dications $\mathbf{3}^{2+}$ in the triplet state. b) Oligomeric TTF vinylogues obtained upon oxidation of compounds **3**.

wave cathodically shifted in comparison to compounds **3** (see Fig. 6a).

As suggested by the atomic orbital composition of the HOMO (Fig. 4), oxidation of compounds **5** only affects the electron-donor 1,3-dithiol-2-ylidene moiety. For **5a**$^{\bullet+}$, this moiety accumulates a charge of +0.93e and presents a geometry similar to that obtained for the dithioles of **3a**$^{2+}$ (Fig. 7c). In a similar way, reduction of compounds **5** mainly affects the electron-acceptor $C(CN)_2$ group, but it also introduces noticeable changes in the pyridine ring. For **5a**$^{\bullet-}$, the $C(CN)_2$ group has a charge of −0.66e and the pyridine ring accumulates a charge of −0.41e. The energy required to oxidize compound **5a** to the radical cation in CH_2Cl_2 solution was calculated to be 6.00 eV.[28] This value is similar to that computed for **4a** (5.97 eV), thus justifying the almost identical oxidation potentials measured for **4a** and **5a** (see Table 1) and is slightly higher in energy than that obtained for **3a** (5.69 eV). All these values are larger than those calculated at the same theoretical level for TTF (5.12 eV) and exTTF (5.14 eV) in agreement with the higher oxidation potentials measured for compounds **3–5** (see Table 1).

The unpaired electron in **5a**$^{\bullet+}$ is mainly localized on the vinylene C3 atom which has a maximum spin density of +0.48 similar to that found for **3a**$^{2+}$ and in accord with the radical species formulated in Scheme 2. Fig. 9a displays the minimum-energy conformation calculated for the TTF vinylogue **6a** resulting from the dimerization of **5a**$^{\bullet+}$ after deprotonation (see Scheme 2). The steric interactions due to the bulky substituents attached to the central conjugated moiety prevent the TTF vinylogue from being planar. The neutral dimer shows a severely distorted structure in which the dithiole rings adopt a cisoid disposition forming a dihedral angle of 54.8° with respect to the central single bond. The structure predicted is similar to those experimentally reported for substituted TTF vinylogues from X-ray crystallographic analysis.[24,29–31]

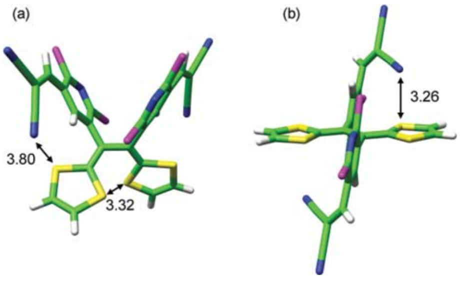

Fig. 9 Minimum-energy conformations calculated at the B3P86/6-31G** level for compound **6a** in the neutral state (a) and as a dication (b). Interatomic distances are given in Å.

Oxidation strongly affects the structure of the dimer **6a**. Contrary to the twisted conformation found for the neutral form, the TTF vinylogue core adopts an almost planar structure in the radical cation and the dication with the pyridine substituents perpendicularly oriented (C_i structure, see Fig. 9b for the dication). The conformational change is due to the modifications occurred on the conjugated system $S_2C{=}C{-}C{=}CS_2$ whose carbon–carbon bond lengths are inverted upon oxidation changing from 1.370 and 1.471 Å in the neutral system to 1.409 and 1.414 Å in the radical cation and to 1.455 and 1.378 Å in the dication. The energy required to oxidize compound **6a** to the radical cation in CH_2Cl_2 solution was calculated to be 5.46 eV. This value is smaller than those computed for **4a** (5.97 eV) and **5a** (6.00 eV) and explains the lower oxidation potential measured for the dimers (see Table 1). Compared with the unsubstituted TTF vinylogue, for which a fully planar structure is predicted and the oxidation to the radical cation costs 4.94 eV at the B3P86/6-31G** level, the dimers of compounds **4** and **5** present higher oxidation potentials due to the conjugation inhibition associated with their highly distorted structures.

Conclusions

In summary, we report on the synthesis of a new family of π-extended TTF donors (**3**) and push–pull analogues (**4** and **5**), in which an electron-defficient pyridine bridge connects the electroactive units (1,3-dithiole rings and 2,2-dicyanovinyl groups). In contrast to many other π-extended TTF derivatives, electrochemical investigations on compounds **3** show the appearance of two oxidation waves. This finding reveals that the two 1,3-dithiole rings do not behave independently despite their *meta* position on the pyridine bridge. Successive oxidative scans evidence an electrochemical–chemical–electrochemical (ECE) process to yield oligomeric TTF vinylogues. A similar electrochemical behaviour is observed for the D–π–A hybrids **4** and **5**. Theoretical calculations—performed at the B3P86/6-31G** level—support these findings and show that, in the oxidation process of donors **3**, electrons are equally extracted from both dithiole rings. The biradical structure predicted for $\mathbf{3}^{2+}$ is proposed to be responsible for the ECE process resulting in the oligomeric TTF-vinylogue. Theoretical calculations show that the ECE oxidative process undergone by hybrids **5** results in the formation of a highly distorted dimeric TTF-vinylogue. The oxidation of such dimers to form dication species strongly affects their structure and the TTF vinylogue core adopts a nearly planar geometry with the pyridine units perpendicularly oriented.

Experimental

General

All solvents were dried and distilled according to standard procedures. Reagents were used as purchased. Compound **1**[21] and phosphonate esters **2a–c**[22] were obtained by previously reported procedures. All air-sensitive reactions were carried out under an argon atmosphere. Flash chromatography was performed using silica gel (Merck, Kiesegel 60, 230–240 mesh or Scharlau 60, 230–240 mesh). Analytical thin layer chromatography (TLC) was performed using aluminium coated Merck Kieselgel 60 F254 plates. Melting points were determined on a Gallenkamp apparatus. NMR spectra were recorded on Varian XL-300 (^{1}H: 300 MHz; ^{13}C: 75 MHz) spectrometer at 298 K using partially deuterated solvents as internal standards. Coupling constants (J) are denoted in Hz and chemical shifts (δ) in ppm. Multiplicities are denoted as follows: s = singlet, d = doublet. IR spectra were recorded on a Perkin-Elmer 257. UV-Vis spectra were recorded in a Varian Cary 50 spectrophotometer by using CH_2Cl_2 as solvent. Mass spectra by electronic impact (EI) were recorded on a HP1100MSD spectrometer. Electrochemical measurements were performed on an Autolab PGStat 30 equipment using a three electrode configuration system. The measurements were carried out using a CH_2Cl_2 solution 0.1 M in tetrabutylammonium perchlorate (TBAClO$_4$). A glassy carbon electrode (3 mm diameter) was used as the working electrode and a platinum wire and an Ag/AgNO$_3$ electrode were employed as the counter and the reference electrode, respectively. Both the counter and the reference electrodes were directly immersed in the electrolyte solution. The surface of the working electrode was polished with commercial alumina prior to use. Solutions were stirred and deaerated by bubbling argon for a few minutes prior to each voltammetric measurement. Unless otherwise specified the scan rate was 100 mV s^{-1}.

Computational details

All theoretical calculations were carried out within the DFT approach using the C.02 revision of the Gaussian 03 program package.[32] DFT calculations were performed using Becke's three-parameter B3P86 exchange–correlation functional[33] and the 6-31G** basis set.[34] The B3P86 functional has been recognized as providing equilibrium geometries for sulfur-containing compounds in better accord with experimental data and *ab initio* post-Hartree–Fock (HF) calculations than the more widely used B3LYP functional.[35] The radical cations were treated as open-shell systems and were computed using spin-unrestricted UB3P86 wavefunctions. Vertical electronic excitation energies were determined by means of the TDDFT approach.[36] Numerous hitherto reported applications indicate that TDDFT employing current exchange–correlation functionals performs significantly better than HF-based single-excitation theories for the low-lying valence excited states. Net atomic charges were calculated using the NPA analysis[37] included in the natural bond orbital (NBO) algorithm proposed by Weinhold and coworkers.[38] Solvent effects were considered within the SCRF (self-consistent-reaction-field) theory using the polarized continuum model (PCM) approach to model the interaction with the solvent.[39] The PCM model considers the solvent as a continuous medium with a dielectric constant ε and represents the solute by means of a cavity built with a number of interlaced spheres.[40]

General procedure for the synthesis of compounds 3a–c

n-Butyllithium (1.6 M, 5.1 mmol) was added dropwise to a solution of the corresponding phosphonate ester **2a–c** (5 mmol) in dry THF at −78 °C under argon atmosphere and the resulting mixture was stirred for 30 minutes at −78 °C. After that, a solution of bis-aldehyde **1** (1 mmol) in dry THF was added. The resulting mixture was stirred at −78 °C for 2 h and then allowed to attain room temperature for 12 h. Evaporation of the solvent gave a yellowish residue which was dissolved in CH_2Cl_2 and then washed with water, dried (MgSO$_4$) and concentrated *in vacuo.* The product was purified by column chromatography (silica gel, hexane–CH_2Cl_2).

3,5-Bis[(1,3-dithiol-2-ylidene)methyl]-2,6-dichloropyridine (3a). (33%); mp 216–219 °C (Found: C, 41.69; H, 1.96; N, 3.74. $C_{13}H_7Cl_2NS_4$ requires C, 41.49; H, 1.86; N, 3.72%); ν_{max}(KBr)/cm^{-1} 3060, 2920, 2840, 1560, 1520, 1490, 1380, 1220, 1100, 1040, 930, 820, 760 and 650; δ_H(300 MHz, CDCl$_3$) 6.38 (2H, dd, J 6.66 and 1.5), 6.48 (2H, dd, J 6.66 and 1.5), 6.76 (2H, d, J 1.5), 7.85 (1H, s); δ_C(75 MHz, CDCl$_3$) 107.62, 128.76, 129.59, 130.92, 139.51, 142.92; UV-Vis (CH_2Cl_2) λ_{max} (nm): 232, 370. m/z (EI) 375 (M$^+$).

3,5-Bis[(4,5-bis(methylthio)-1,3-dithiol-2-ylidene)methyl]-2,6-dichloropyridine (3b). (40%); mp 166–169 °C (Found: C, 36.60; H, 2.90; N, 2.55. $C_{17}H_{15}Cl_2NS_8$ requires C, 36.42; H, 2.70; N, 2.50%). ν_{max}(KBr)/cm^{-1} 2940, 2880, 1570, 1560, 1500, 1480, 1460, 1430, 1380, 1220, 1100, 970, 960, 940, 890, 850, 810, 790, 740 and 720; δ_H(300 MHz, CDCl$_3$) 2.46 (6H, s), 2.48 (6H, s), 6.66 (2H, s), 7.65 (1H, s); ^{13}C NMR (CDCl$_3$, 75 MHz) δ: 19.05, 19.37, 107.60, 128.79, 129.64, 131.03, 139.47, 142.89; UV-Vis (CH_2Cl_2) λ_{max} (nm): 232, 284, 385. m/z (EI) 559 (M$^+$).

3,5-Bis[(4,5-bis(ethylenedithio)-1,3-dithiol-2-ylidene)methyl]-2,6-dichloropyridine (3c). (48%); mp > 350 °C (decomp.) (Found: C, 36.99; H, 2.10; N, 2.60. $C_{17}H_{11}Cl_2NS_8$ requires C, 36.68; H, 1.99; N, 2.52%). ν_{max}(KBr)/cm^{-1} 2930, 2840, 1580, 1560, 1520, 1490, 1410, 1380, 1290, 1220, 1100, 930, 890 and 800; δ_H(300 MHz, CDCl$_3$) 3.36 (8H, s), 6.67 (2H, s), 7.61 (1H, s); UV-Vis (CH_2Cl_2) λ_{max} (nm): 232, 265, 398. m/z (EI) 557 (M$^+$).

General procedure for the synthesis of aldehydes 4a–c

n-Butyllithium (1.6 M, 1.1 mmol) was added dropwise to a solution of the corresponding phosphonate ester **2a–c** (1 mmol) in dry THF at −78 °C under argon atmosphere and the resulting mixture was stirred for 30 minutes at −78 °C. After that, a solution of bis-aldehyde **1** (1 mmol) in dry THF was added. The resulting mixture was stirred at −78 °C for 2 h and then allowed to attain room temperature for 12 h. Evaporation of the solvent gave a yellowish residue which was dissolved in CH_2Cl_2 and then washed with water, dried (MgSO$_4$) and concentrated *in vacuo.* The product was purified by column chromatography (silica gel, hexane–CH_2Cl_2).

5-[(1,3-Dithiol-2-ylidene)methyl]-2,6-dichloropyridine-3-carbaldehyde (4a). (28%); mp 187–190 °C (Found: C, 41.59; H, 1.89; N, 4.86. $C_{10}H_5Cl_2NOS_2$ requires C, 41.39; H, 1.74; N, 4.83%). ν_{max}(KBr)/cm^{-1}: 3080, 2950, 2860, 1700, 1560, 1520, 1400, 1380, 1330, 1260, 1205, 1110, 1090, 1040, 940, 890, 820, 800, 750, 730, 680, 660, 640 and 630; δ_H(300 MHz, CDCl$_3$) 6.45 (1H, dd, J 6.9 and 1.2), 6.55 (1H, d, J 6.9), 6.79 (1H, s), 8.29 (1H, s), 10.41 (1H, s); δ_C(75 MHz, CDCl$_3$) 103.69, 117.39, 118.85, 127.29, 131.49, 133.48, 188.22; UV-Vis (CH_2Cl_2) λ_{max} (nm): 234, 277, 389, 488. *m/z* (EI) 289 (M^+).

5-[(4,5-Bis(methylthio)-1,3-dithiol-2-ylidene)methyl]-2,6-dichloropyridine-3-carbaldehyde (4b). (28%); mp 183–185 °C (Found: C, 37.77; H, 2.79; N, 3.23. $C_{12}H_9Cl_2NOS_4$ requires C, 37.70; H, 2.37; N, 3.66%). ν_{max}(KBr)/cm^{-1} 1790, 1580, 1560, 1490, 1430, 1390, 1370, 1330, 1190, 1100, 1040, 990, 930, 880, 810, 740, 720 and 640; δ_H(300 MHz, $CDCl_3$) 2.44 (3H, s), 2.48 (3H, s), 6.68 (1H, s), 8.17 (1H, s), 10.40 (1H, s); δ_C(75 MHz, $CDCl_3$) 19.08, 19.20, 105.57, 127.32, 130.99, 134.24, 138.77, 142.56, 146.86, 188.04; UV-Vis (CH_2Cl_2) λ_{max} (nm): 232, 324, 389, 551. *m/z* (EI) 381 (M^+).

5-[(4,5-Bis(ethylenedithio)-1,3-dithiol-2-ylidene)methyl]-2,6-dichloropyridine-3-carbaldehyde (4c). (35%); mp 214–215 °C (Found: C, 38.10; H, 2.00; N, 3.52. $C_{12}H_7Cl_2NOS_4$ requires C, 37.90; H, 1.86; N, 3.68%). ν_{max}(KBr)/cm^{-1} 2980, 2950, 2880, 1700, 1590, 1570, 1520, 1470, 1390, 1370, 1340, 1200, 1230, 1210, 1180, 1130, 1110, 1080, 1040, 990, 950, 890, 800, 760 and 740; δ_H(300 MHz, $CDCl_3$) 3.67 (4H, s), 6.71 (1H, s), 8.15 (1H, s), 10.40 (1H, s); UV-Vis (CH_2Cl_2) λ_{max} (nm): 248, 282, 410, 592. *m/z* (EI) 379 (M^+).

General procedure for the synthesis of 2,2-dicyanovinyls 5a–c

To a solution of the corresponding aldehyde **4a–c** (2 mmol) in toluene (200 mL), malononitrile (4 mmol), ammonium acetate (110 mg) and acetic acid (5 mL) were added. The resulting mixture was refluxed for 24 h with azeotropic elimination of water by using a Dean–Stark apparatus. After this time, the mixture was allowed to reach room temperature and the solvent was removed under reduced pressure. The final D–π–A compounds were purified by column chromatography by using a hexane–CH_2Cl_2 as eluent.

2,6-Dichloro-5-(2′,2′-dicyanovinyl)-3-[(1,3-dithiol-2-ylidene)-methyl]pyridine (5a). (65%); mp 172–175 °C (Found: C, 46.55; H, 1.79; N, 12.20. $C_{13}H_5Cl_2N_3S_2$ requires C, 46.15; H, 1.48; N, 12.43%). ν_{max}(KBr)/cm^{-1} 2924, 2237, 1559, 1520, 1506, 1500, 1383, 1102 and 668; δ_H(300 MHz, $CDCl_3$) 6.50 (1H, dd, *J* 6.6 and 1.5), 6.57 (1H, d, *J* 6.6), 6.79 (1H, s), 8.15 (1H, s), 8.41 (1H, s); δ_C(75 MHz, $CDCl_3$) 102.96, 112.63, 117.82, 119.10, 128.68, 129.28, 129.28, 130.75, 131.41, 132.01, 132.63, 148.25, 153.69; UV-Vis (CH_2Cl_2) λ_{max} (nm): 243, 322, 484. *m/z* (EI) 337 (M^+).

2,6-Dichloro-5-(2′,2′-dicyanovinyl)-3-[4,5-bis(methylthio)-(1,3-dithiol-2-ylidene)methy)]pyridine (5b). (70%); mp 169–171 °C (Found: C, 42.03; H, 2.33; N, 10.20. $C_{15}H_9Cl_2N_3S_4$ requires C, 41.86; H, 2.11; N, 9.76%). ν_{max}(KBr)/cm^{-1} 2923, 2852, 2232, 1595, 1580, 1560, 1544, 1488, 1383, 1200, 1179, 1065, 971, 910, 879 and 786; δ_H(300 MHz, $CDCl_3$) 2.47 (6H, s), 6.67 (1H, s), 8.14 (1H, s), 8.34 (1H, s); δ_C(75 MHz, $CDCl_3$) 29.58, 104.53, 111.20, 112.60, 124.33, 130.98, 132.68, 144.11, 151.47, 153.45; UV-Vis (CH_2Cl_2) λ_{max} (nm): 232, 287, 410, 555. *m/z* (EI) 429 (M^+).

2,6-Dichloro-5-(2′,2′-dicyanovinyl)-3-[4,5-bis(ethylendithio)-(1,3-dithiol-2-ylidene)methyl]pyridine (5c). (68%); mp 179–182 °C (Found: C, 42.33; H, 1.80; N, 9.69. $C_{15}H_7Cl_2N_3S_4$ requires C, 42.06; H, 1.65; N, 9.81%). Found: ν_{max}(KBr)/cm^{-1} 2990, 2960, 2890, 2240, 1590, 1520, 1480, 1420, 1400, 1310, 1050 and 940; δ_H(300 MHz, $CDCl_3$) 3.37 (4H, s), 6.69 (1H, s), 8.14 (1H, s), 8.31 (1H, s); δ_C(75 MHz, $CDCl_3$) 29.66, 104.59, 111.24, 112.66, 142.44, 134.28, 142.21, 144.07, 145.45, 151.64, 153.64; UV-Vis (CH_2Cl_2) λ_{max} (nm): 252, 292, 422, 424, 564. *m/z* (EI) 427 (M^+).

Acknowledgements

This work has been supported by the Ministerio de Educación y Ciencia (MEC) of Spain (grants BQU2003-05111, CTQ2005-02609/BQU and CTQ2006-14987-C02-02/BQU), by the Comunidad de Madrid (P-PPQ-000225-0505) and by the Generalitat Valenciana. M.A.H. would like to thank the MEC for a “Ramón y Cajal” contract.

Notes and references

1 (*a*) A. Nitzan and M. A. Ratner, *Science*, 2003, **300**, 1384; (*b*) J. R. Heath, J. F. Stoddart and R. S. Williams, *Science*, 2004, **303**, 1136; (*c*) R. A. Wassel and C. B. Gorman, *Angew. Chem., Int. Ed.*, 2004, **43**, 5120; (*d*) R. A. Wassel, Special issue on *Organic Electronics*, *Chem. Mater.*, 2004, **16**, 4381; (*e*) R. L. Carroll and C. B. Gorman, *Angew. Chem., Int. Ed.*, 2002, **41**, 4378; (*f*) J. M. Tour, *Acc. Chem. Res.*, 2000, **33**, 791.

2 (*a*) I. W. Tam, J. Yan and R. Breslow, *Org. Lett.*, 2006, **8**, 183; (*b*) G. de la Torre, F. Giacalone, J. L. Segura, N. Martín and D. M. Guldi, *Chem.–Eur. J.*, 2005, **11**, 1267; (*c*) S. Xiao, M. Myers, Q. Miao, S. Sanaur, K. Pang, M. L. Steigerwald and C. Nuckolls, *Angew. Chem., Int. Ed.*, 2005, **44**, 7390; (*d*) T. Oike, T. Kurata, K. Takimiya, T. Otsubo, Y. Aso, H. Zhang, Y. Araki and O. Ito, *J. Am. Chem. Soc.*, 2005, **127**, 15372; (*e*) F. Giacalone, J. L. Segura, N. Martín and D. M. Guldi, *J. Am. Chem. Soc.*, 2004, **126, 126**, 5340; (*f*) E. A. Weiss, M. J. Ahrens, L. E. Sinks, A. V. Gusev, M. A. Ratner and M. R. Wasielewski, *J. Am. Chem. Soc.*, 2004, **126**, 5577.

3 (*a*) J. Andrasson, Y. Terazono, B. Albinsson, T. A. Moore, A. L. Moore and D. Gust, *Angew. Chem., Int. Ed.*, 2005, **44**, 7591; (*b*) F. M. Raymo and S. Giordani, *J. Am. Chem. Soc.*, 2002, **124**, 2004; (*c*) A. Credi, V. Balzani, S. J. Langford and J. F. Stoddart, *J. Am. Chem. Soc.*, 1997, **119**, 2679.

4 (*a*) B. L. Feringa, *Molecular Switches*, Wiley-VCH, Weinheim, 2001; (*b*) F. M. Raymo and M. Tomasulo, *Chem.–Eur. J.*, 2006, **12**, 3186; (*c*) C. Trieflinger, K. Rurack and J. Daub, *Angew. Chem., Int. Ed.*, 2005, **44**, 2288; (*d*) D. A. Leigh, M. A. F. Morales, E. M. Pérez, J. K. Y. Wong, C. G. Saiz, A. M. Z. Slawin, A. J. Carmichael, D. M. Haddleton, A. M. Brouwer, W. J. Buma, G. W. H. Wurpel, S. León and F. Zerbetto, *Angew. Chem., Int. Ed.*, 2005, **44**, 3062; (*e*) S. Kang, S. A. Vignon, H.-R. Tseng and J. F. Stoddart, *Chem.–Eur. J.*, 2004, **10**, 2555.

5 (*a*) N. Stingelin-Stutzmann, E. Smits, H. Wondergem, C. Tanase, P. Blom, P. Smith and D. De Leeuw, *Nat. Mater.*, 2005, **4**, 601; (*b*) S. Kobayashi, T. Nishikawa, T. Takenobu, S. Mori, T. Shimoda, T. Mitani, H. Shimotani, N. Yoshimoto, S. Ogawa and Y. Iwasa, *Nat. Mater.*, 2004, **3**, 317; (*c*) S. Kubatkin, A. Danilov, M. Hjort, J. Cornil, J.-L. Brédas, N. Stuhr-Hansen, P. Hedegård and T. Bjørnholm, *Nature*, 2003, **425**, 698.

6 (*a*) V. A. Azov, A. Schlegel and F. Diederich, *Angew. Chem., Int. Ed.*, 2005, **44**, 4635; (*b*) X. Xiao, L. A. Nagahara, A. M. Rawlett and N. Tao, *J. Am. Chem. Soc.*, 2005, **127**, 9235.

7 Molecular geometry plays a major role in the field of OFETs, in which the best results have been reported for rigid and planar molecules like pentacene and rubrene (see for example: J.-L. Brédas, D. Beljonne, V. Coropceanu and J. Cornil, *Chem. Rev.*, 2004, **104**, 4971), or in the field of molecular switches, in which the stimulus-dependent (pH, temperature, *etc.*) geometry of the molecular components gives rise to bistable conformations with different properties (see reference 4).

8 (*a*) D. F. Perepichka and M. R. Bryce, *Angew. Chem., Int. Ed.*, 2005, **44**, 5370; (*b*) M. Bendikov, F. Wudl and D. F. Perepichka, *Chem. Rev.*, 2004, **104**, 4891.

9 (*a*) G. Sonmez, C. K. F. Shen, Y. Rubin and F. Wudl, *Angew. Chem., Int. Ed.*, 2004, **43**, 1498; (*b*) *Handbook of Conducting Polymers*, ed. T. A. Skotheim, R. L. Elsenbaumer and J. R. Reynolds, Marcel Dekker, New York, 2nd edn, 1998.

10 F. Wudl, G. M. Smith and E. J. Hufnagel, *J. Chem. Soc. D*, 1970, 1453.

11 For recent reviews on TTF chemistry, see: (*a*) J. L. Segura and N. Martín, *Angew. Chem., Int. Ed.*, 2001, **40**, 1372; (*b*) M. R. Bryce,

J. Mater. Chem., 2000, **10**, 589; (*c*) M. B. Nielsen, C. Lomholt and J. Becher, *Chem. Soc. Rev.*, 2000, **29**, 153.

12 (*a*) M. Sato, N. C. Gonnella and M. P. Cava, *J. Org. Chem.*, 1979, **44**, 930; (*b*) A. J. Moore, M. R. Bryce, D. J. Ando and M. B. Hursthouse, *J. Chem. Soc., Chem. Commun.*, 1991, 320; (*c*) J. Roncali, *J. Mater. Chem.*, 1997, **7**, 2307; (*d*) T. Khan, P. J. Skabara, P. Frère, M. Allain, S. J. Coles and M. B. Hursthouse, *Tetrahedron Lett.*, 2004, **45**, 2535.

13 (*a*) T. K. Hansen, M. V. Lakshmikantham, M. P. Cava, R. E. Niziurski-Mann, F. Jensen and J. Becher, *J. Am. Chem. Soc.*, 1992, **114**, 5035; (*b*) P. Frère, M. Allain, M. Elandaloussi, E. Levillain, F. X. Sauvage, A. Riou and J. Roncali, *Chem.–Eur. J.*, 2002, **8**, 784; (*c*) E. Aqad, M. V. Lakshmikantham, M. P. Cava, R. M. Metzger and V. Khodorkhovsky, *J. Org. Chem.*, 2005, **70**, 768.

14 (*a*) Y. Yamashita, Y. Kobayashi and T. Miyashi, *Angew. Chem., Int. Ed. Engl.*, 1989, **28**, 1052; (*b*) M. R. Bryce, A. J. Moore, M. Hasan, G. J. Ashwell, A. T. Fraser, W. Clegg, M. B. Hursthouse and A. I. Karaulov, *Angew. Chem., Int. Ed. Engl.*, 1990, **29**, 1450; (*c*) N. Martín, L. Sánchez, C. Seoane, E. Ortí, P. M. Viruela and R. Viruela, *J. Org. Chem.*, 1998, **63**, 1268; (*d*) M. C. Díaz, B. M. Illescas, N. Martín, R. Viruela, P. M. Viruela, E. Ortí, O. Brede, I. Zilbermann and D. M. Guldi, *Chem.–Eur. J.*, 2004, **10**, 2067.

15 The combination of acceptor units of different natures with TTF or π-extended TTF derivatives by using a σ-spacer is an active research field, especially for the preparation of molecular rectifiers (for recent examples, see: (*a*) G. Ho, J. R. Heath, M. Kondratenko, D. F. Perepichka, K. Arseneault, M. Pézolet and M. R. Bryce, *Chem.–Eur. J.*, 2005, **11**, 2914; (*b*) D. F. Perepichka, M. R. Bryce, C. Pearson, M. C. Petty, E. J. L. McInnes and J. P. Zhao, *Angew. Chem., Int. Ed.*, 2003, **42**, 4636; (*c*) D. F. Perepichka, M. R. Bryce, I. F. Perepichka, S. B. Lyubchik, N. Godbert, C. A. Christensen, A. S. Batsanov, E. Levillain, E. J. L. McInnes and J. P. Zhao, *J. Am. Chem. Soc.*, 2002, **124**, 14227) or artificial photosynthetic systems (see, for example: a); N. Martín, L. Sánchez, B. Illescas and I. Pérez, *Chem. Rev.*, 1998, **98**, 2527; b); M. Segura, L. Sánchez, J. de Mendoza, N. Martín and D. M. Guldi, *J. Am. Chem. Soc.*, 2003, **125**, 15093; c); L. Sánchez, M. Sierra, N. Martín, D. M. Guldi, M. M. Wienk and R. A. J. Janssen, *Org. Lett.*, 2005, **7**, 1691; d); D. M. Guldi, F. Giacalone, G. de la Torre, J. L. Segura and N. Martín, *Chem.–Eur. J.*, 2005, **11**, 7199.

16 (*a*) *Materials for Nonlinear Optics: Chemical Perspectives*, ed. S. R. Marder, G. D. Stucky and J. E. Sohn, ACS Symposium Series, American Chemical Society, Washington, DC, 1991, vol. 455; (*b*) *Nonlinear Optics of Organic Molecules and Polymers*, ed. H. S. Nalwa and S. Miyata, CRC Press, Boca Raton, FL, 1997; (*c*) J. J. Wolf and R. Wortmann, *Adv. Phys. Org. Chem.*, 1999, **32**, 121.

17 (*a*) M. González, J. L. Segura, C. Seoane, N. Martín, J. Garín, J. Orduna, R. Alcalá, B. Villacampa, V. Hernández and J. T. López, *J. Org. Chem.*, 2001, **66**, 8872; (*b*) B. Insuasty, C. Atienza, C. Seoane, N. Martín, J. Garín, J. Orduna, R. Alcalá and B. Villacampa, *J. Org. Chem.*, 2004, **69**, 6986; (*c*) R. Andreu, M. J. Blesa, L. Carrasquer, J. Garín, J. Orduna, B. Villacampa, R. Alcalá, J. Casado, M. C. Ruiz Delgado, J. T. López Navarrete and M. Allain, *J. Am. Chem. Soc.*, 2005, **127**, 8835.

18 (*a*) A. S. Batsanov, M. R. Bryce, M. A. Coffin, A. Green, R. E. Hester, J. A. K. Howard, I. K. Lednev, N. Martín, A. J. Moore, J. N. Moore, E. Ortí, L. Sánchez, M. Savirón, P. M. Viruela, R. Viruela and T.-Q. Ye, *Chem.–Eur. J.*, 1998, **4**, 2580; (*b*) S. Amriou, C. Wang, A. S. Batsanov, M. R. Bryce, D. F. Perepichka, E. Ortí, R. Viruela, J. Vidal-Gancedo and C. Rovira, *Chem.–Eur. J.*, 2006, **12**, 3389.

19 A. L. Thompson, T.-S. Ahn, K. R. J. Thomas, S. Thayumanavan, T. J. Martínez and C. J. Bardeen, *J. Am. Chem. Soc.*, 2005, **127**, 16348.

20 (*a*) A. Lutzen, M. Hapke, H. Saats and J. Bunzen, *Eur. J. Org. Chem.*, 2003, 3948; (*b*) T. Tagata and M. Nishida, *J. Org. Chem.*, 2003, **68**, 9412; (*c*) M. Schlosser and T. Rausis, *Helv. Chim. Acta*, 2005, **88**, 1240; (*d*) A. Abad, C. Agullo, A. C. Cunat and C. Vilanova, *Synthesis*, 2005, 915.

21 A. Guzmán, M. Romero, M. L. Maddox and J. M. Muchowski, *J. Org. Chem.*, 1990, **55**, 5793.

22 A. J. Moore and M. R. Bryce, *Synthesis*, 1991, 26.

23 W. Koch and M. C. Holthausen, *A Chemist's Guide to Density Functional Theory*, Wiley-VCH, Weinheim, Germany, 2000.

24 (*a*) D. Lorcy, R. Carlier, A. Robert, A. Tallec, P. Le Maguerès and L. Ouahab, *J. Org. Chem.*, 1995, **60**, 2443; (*b*) S. González, N. Martín, L. Sánchez, J. L. Segura, C. Seoane, I. Fonseca, F. H. Cano, J. Sedó, J. Vidal-Gancedo and C. Rovira, *J. Org. Chem.*, 1999, **64**, 3498; (*c*) M. Guerro, R. Carlier, K. Boubekeur, D. Lorcy and P. Hapiot, *J. Am. Chem. Soc.*, 2003, **125**, 3159.

25 (*a*) P. Frère and P. J. Skabara, *Chem. Soc. Rev.*, 2005, **34**, 69; (*b*) R. Berridge, P. J. Skabara, R. Andreu, J. Garín, J. Orduna and M. Torra, *Tetrahedron Lett.*, 2005, **34**, 7871; (*c*) M. Fourmigué, I. Johannsen, K. Boubekeur, C. Nelson and P. Batail, *J. Am. Chem. Soc.*, 1993, **115**, 3752.

26 P. Hapiot, D. Lorcy, A. Tallec, R. Carlier and A. Robert, *J. Phys. Chem.*, 1996, **100**, 14823.

27 Geometry optimizations were performed both for the isolated molecule and in the presence of the solvent ($\mathrm{CH_2Cl_2}$). Calculations showed that the solvent has a very small effect on the geometrical parameters, the maximum differences being of 0.005 Å for the dication species.

28 Adiabatic ionization energy calculated as the difference between the total energies obtained for **5a**$^{\cdot+}$ and **5a** at their optimized geometries in the presence of the $\mathrm{CH_2Cl_2}$ solvent.

29 H. Hopf, M. Kreutzer and P. G. Jones, *Angew. Chem., Int. Ed. Engl.*, 1991, **30**, 1127.

30 (*a*) A. Ohta and Y. Yamashita, *J. Chem. Soc., Chem. Commun.*, 1995, 1761; (*b*) Y. Yamashita, M. Tomura, M. Braduz Zaman and K. Imaeda, *Chem. Commun.*, 1998, 1657.

31 A. J. Moore, M. R. Bryce, P. J. Skabara, A. S. Batsanov, L. M. Goldenberg and J. A. K. Howard, *J. Chem. Soc., Perkin Trans. 1*, 1997, 3443.

32 *Gaussian 03, Revision C.02*, M. J. Frisch, G. W. Trucks, H. B. Schlegel, G. E. Scuseria, M. A. Robb, J. R. Cheeseman, Jr., J. A. Montgomery, T. Vreven, K. N. Kudin, J. C. Burant, J. M. Millam , S. S. Iyengar, J. Tomasi, V. Barone, B. Mennucci, M. Cossi, G. Scalmani, G. Rega, G. A. Petersson, H. Nakatsuji, M. Hada, M. Ehara, K. Toyota, R. Fukuda, J. Hasegawa, M. Ishida, T. Nakajima, Y. Honda, O. Kitao, H. Nakai, M. Klene, X. Li, J. E. Knox, H. P. Hratchian, J. B. Cross, V. Bakken, C. Adamo, J. Jaramillo, R. Gomperts, R. E. Stratmann, O. Yazyev, A. J. Austin, R. Cammi, C. Pomelli, J. W. Ochterski, P. Y. Ayala, K. Morokuma, G. A. Voth, P. Salvador, J. J. Dannenberg, V. G. Zakrzewski, S. Dapprich, A. D. Daniels, M. C. Strain, O. Farkas, D. K. Malick, A. D. Rabuck, K. Raghavachari, J. B. Foresman, J. V. Ortiz, Q. Cui, A. G. Baboul, S. Clifford, J. Cioslowski, B. B. Stefanov, G. Liu, A. Liashenko, P. Piskorz, I. Komaromi, R. L. Martin, D. J. Fox, T. Keith, M. A. Al-Laham, C. Y. Peng, A. Nanayakkara, M. Challacombe, P. M. W. Gill, B. Johnson, W. Chen, M. W. Wong, C. Gonzalez and J. A. Pople, Gaussian, Inc.: Wallingford CT, 2004.

33 J. P. Perdew, *Phys. Rev. B: Condens. Matter Mater. Phys.*, 1986, **33**, 8822.

34 M. M. Francl, W. J. Pietro, W. J. Hehre, J. S. Binkley, M. S. Gordon, D. J. Defrees and J. A. Pople, *J. Chem. Phys.*, 1982, **77**, 3654.

35 (*a*) P. M. Viruela, R. Viruela, E. Ortí and J.-L. Brédas, *J. Am. Chem. Soc.*, 1997, **119**, 1360; (*b*) R. Liu, X. Zhou and H. Kasmai, *Spectrochim. Acta, Part A*, 1997, **53**, 1241; (*c*) J. A. Altmann, N. C. Handy and V. E. Ingamells, *Mol. Phys.*, 1997, **92**, 339.

36 (*a*) E. Runge and E. K. U. Gross, *Phys. Rev. Lett.*, 1984, **52**, 997; (*b*) E. K. U. Gross and W. Kohn, *Adv. Quantum Chem.*, 1990, **21**, 255; (*c*) E. K. U. Gross, C. A. Ullrich and U. J. Gosssman, *Density Functional Theory*, ed. E. K. U. Gross and R. M. Driezler, Plenum Press, New York, 1995, p. 149; (*d*) M. E. Casida, *Recent Advances in Density Functional Methods, Part I*, ed. D. P. Chong, World Scientific, Singapore, 1995, p. 155.

37 (*a*) A. E. Reed and F. Weinhold, *J. Chem. Phys.*, 1983, **78**, 4066; (*b*) A. E. Reed, R. B. Weinstock and F. Weinhold, *J. Chem. Phys.*, 1985, **83**, 735.

38 A. E. Reed, L. A. Curtiss and F. Weinhold, *Chem. Rev.*, 1988, **88**, 899.

39 (*a*) J. Tomasi and M. Persico, *Chem. Rev.*, 1994, **94**, 2027; (*b*) C. S. Cramer and D. G. Truhlar, *Solvent Effects and Chemical Reactivity*, ed. O. Tapia and J. Bertrán, Kluwer, Dordrecht, 1996, p. 1.

40 (*a*) S. Miertus, E. Scrocco and J. Tomasi, *Chem. Phys.*, 1981, **55**, 117; (*b*) S. Miertus and J. Tomasi, *Chem. Phys.*, 1982, **65**, 239; (*c*) M. Cossi, V. Barone, R. Cammi and J. Tomasi, *Chem. Phys. Lett.*, 1996, **255**, 327; (*d*) E. Cances, B. Mennucci and J. Tomasi, *J. Chem. Phys.*, 1997, **107**, 3032; (*e*) V. Barone, M. Cossi and J. Tomasi, *J. Comput. Chem.*, 1998, **19**, 404; (*f*) M. Cossi, G. Scalmani, N. Rega and V. Barone, *J. Chem. Phys.*, 2002, **117**, 43.